

Proposed Methodology for Non-Contact Angular Measurement via Computer Vision - PYAXIOMA-JH

JOSEPH HAVENS ¹ AND LUCCIANA M. CACERES HOLGADO  ¹

¹*Department of Physics and Astronomy, University of Kansas, Lawrence, KS 66045, USA*

ABSTRACT

I present a method for measuring angular displacement of an object using computer vision and optical flow, without requiring physical contact. By identifying colored markers and tracking their displacement through video frames captured with a standard laptop camera (in this instance my mid-2020 M1 MacBook Pro), I compute real-time angular motion. The method uses color segmentation, morphological filtering, Hough circle detection, and frame differencing to track movement. This low-cost setup, built entirely in Python with OpenCV, offers a proof-of-concept for future experimental use and calibration.

1. INTRODUCTION

Non-contact measurement methods are crucial for systems where physical probes interfere with function. Measuring angular position traditionally requires rotary encoders or potentiometers, which are invasive or impractical for rotating or delicate components. Recent advances in computer vision allow accurate motion tracking with standard cameras, making optical methods viable for torque analysis.

This work is motivated by a broader need in experimental and applied physics for non-invasive, real-time diagnostic tools that do not compromise the physical behavior of the system being studied. Applications include rotating magnetic systems, precision robotics, small-scale torsion balances, and fragile mechanical systems where attaching sensors is impractical or alters inertial properties. Vision-based systems allow measurements to be taken remotely, with minimal interference and high temporal resolution.

Although several commercial systems exist for motion tracking, they often require expensive multi-camera setups or proprietary software, making them inaccessible to many researchers. PYAXIOMA addresses this by combining open-source libraries with minimal hardware demands, offering reproducibility, transparency, and affordability. It leverages real-time image processing and motion segmentation techniques to analyze angular displacement using marker tracking.

Here, I introduce a fascinating, contactless angular measurement method using visual tracking of object rotation. My software PYAXIOMA, officially known as the PYAXIOMA JH method (**P**ython **A**xis of Mag-

netic **O**scillation and **M**otion **A**nalysis as developed by Joseph Havens) employs motion-based tracking and optical flow to compute angular acceleration.

2. METHODOLOGY OVERVIEW

The PYAXIOMA pipeline consists of four main steps:

1. Cue ball detection using Hough circle detection (Yuen et al. 1990) and HSV color detection (Smith 1978)
2. Iterative motion contrast mask using frame differencing (Piccardi 2004) and morphological operations (Gonzalez & Woods 2002)
3. The largest motion contour (see ??) is selected in each iteration, and centroid calculations are employed to detect the black marker (Hu 1962)
4. Finally, I identify the center of the black marker and mark it as

`cx_black, cy_black`

Once the central coordinates of the black marker have been identified and stored, I perform angular calculations. I treat the lines connecting the center of the circle to the black marker and the horizontal as row-vectors, and employ equation 1 below to find the angle, θ , from the horizontal to the black marker.

$$\cos \theta = \frac{A \cdot B}{|A||B|} \quad (1)$$

2.1. Data Storage

Finally, I store angular values in a .csv with the amperage clearly marked. Section 2.7 explains why marking the amperage clearly is important. Alongside the

joe.havens79@ku.edu

lucciana.caceres@ku.edu

recorded angular values, I also store the UTC time of that angle, time elapsed, and a calculated confidence value. I use the UTC time to interpolate data collected using PYAXIOMA LC Method with data from [Caceres Holgado \(2025\)](#), which I will further discuss in Section 2.7.

2.2. Hardware and Video Acquisition

I use a MacBook Pro camera (1080p @ 32 fps) mounted orthogonally to the plane of rotation. A white background aids segmentation, initially a blank poster board provided by Kristin Rennells, but this proved inadequately effective, so a simple piece of paper was used instead. I chose this instead as it was much more flexible and could be placed immediately behind the cue ball where it was needed most.

2.3. Circle Selection and Color Segmentation

Before iterative angle measurements are taken, PYAXIOMA will repeatedly seek to find the cue ball using HSV color detection ([Smith 1978](#)) and Hough Circle Transform ([Yuen et al. 1990](#)). I use HSV segmentation for robust color detection. Morphological filtering removes noise before I pass the mask to Hough circle detection.

2.4. Optical Flow and Marker Detection

When the main processing loop of PYAXIOMA begins, it performs motion detection using a frame differencing approach to isolate dynamic regions of interest. Unlike traditional optical flow techniques that compute pixel-wise displacement fields, PYAXIOMA implements a simplified approximation by subtracting consecutive grayscale frames and applying a binary threshold to the result. This creates a motion mask that highlights pixels which have changed significantly between frames.

The difference mask is then refined using a morphological closing operation with a 5×5 kernel. This operation removes small holes and bridges gaps within the motion regions, allowing cleaner extraction of contiguous contours. The largest contour is assumed to correspond to the moving marker.

A threshold of 1.75 was selected to exclude small or spurious regions of movement. This value was determined empirically by testing the sensitivity of the MacBook Pro's camera under experimental lighting conditions. It effectively eliminated background jitter and isolated only the most significant moving object—usually the black marker used for angular tracking.

Once the motion contour is extracted, its centroid is computed using image moments. The coordinates $(cx_{\text{black}}, cy_{\text{black}})$ define the marker's center, which is then used to compute the angle relative to the cue ball. This

angle is derived by forming a vector from the cue ball's center to the black marker and calculating its angle with respect to a horizontal reference, with quadrant-specific adjustments for directional accuracy.

Because this methodology depends heavily on visible movement, PYAXIOMA does not compute angles when the marker remains stationary between frames. While this is a limitation in terms of detecting steady-state positions, it aligns with the objective of detecting torque-induced motion, which is inherently dynamic.

Figure 1 shows an example of when PYAXIOMA successfully identifies the cue ball and marker and marks both the marker vector and horizontal reference vector. In addition, a box is drawn around the marker representing the largest area on the motion contour, and two small circles can be seen representing where the marker is found. Two additional windows are seen, an optical flow motion mask and a grey-scale feed. These windows yield additional views of the cue ball and marker. Additionally, we also see a green **TRACKING ACTIVE** marker and an angular measurement in the upper left corner.



Figure 1: Example of motion mask generated via frame differencing and morphological filtering. Bright regions correspond to detected movement, typically from the black marker.

2.5. Angle Computation and Directional Adjustment

Once the marker's center is identified, I calculate its angular position relative to the horizontal by forming a vector between the cue ball's center and the black marker. This angle is derived from Eq. 1, with quadrant-specific corrections implemented to ensure angular continuity and directionality.

The angle θ is computed using:

$$\theta = \arccos \left(\frac{B_x}{\sqrt{B_x^2 + B_y^2}} \right) \quad (2)$$

This value is then adjusted depending on which quadrant the marker falls into. If the vector lies in quadrant II or III, the angle is reflected across the vertical axis; if in quadrant IV, the angle is negative. These conditional corrections ensure that the resulting θ provides a full $[-90^\circ, 270^\circ]$ range and avoids wraparound artifacts common in polar calculations.

PYAXIOMA also uses real-time overlay annotations to visualize this vector, aiding debugging and validation. These vectors are drawn directly on the live feed, showing both marker location and direction of rotation.

2.6. Confidence Metric Estimation

To assess the reliability of each angular measurement, PYAXIOMA computes a composite confidence score for each frame. High angular stability, low jerk and angular velocity, and full angular extent were all rewarded with high confidence values. Conversely, erratic angle values, high jerk or angular velocity, or angle values constricted around 90° were all punished with diminished confidence.

For future work, this is a massive section I would like to improve. I find that these calculations are not fully developed and do not yield the exact values that seem reasonable for the conditions. However the shape, as seen in Figure 2, is exactly as expected for these conditions.

Each factor is normalized and weighted, and the final confidence score is clipped between 0 and 1. This value is displayed on the GUI and recorded alongside each timestamped angle for downstream analysis.

2.7. Data Interpolation and Interpretation

When the trial is completed, the OpenCV windows are closed and deleted, and the data is stored in a csv with amperage clearly marked. It is important to mark the amperage since the Amps in the system play a crucial role in the magnetic field induced, changing the torque applied, and thus changing the speed at which the marker moves. A relation of 0.00137 Teslas/Ampere, as noted in the student manual ([Department of Physics and Astronomy 2024](#)), will be helpful both in plots found within [Caceres Holgado \(2025\)](#) as well as calculations within this paper.

We made sure to save the UTC time of each measurement, so that later combination can be done to combine the two 2D projections into a nearly perfect 3D map of the marker's movement. By marking the UTC time, we have a very easy method of aligning our angular data for proper calculations.

3. RESULTS

A series of video trials were conducted at various current levels (amperages), with each run recorded and processed through PYAXIOMA. For each frame, angular position, confidence score, UTC timestamp, and time elapsed were logged.

The system was able to detect angular displacement consistently across most trials. Representative output showed angular motion consistent with theoretical expectations of torque-induced oscillations. Figure 2 shows a typical angular position vs. time curve, and Table 1 presents a subset of the output dataset.

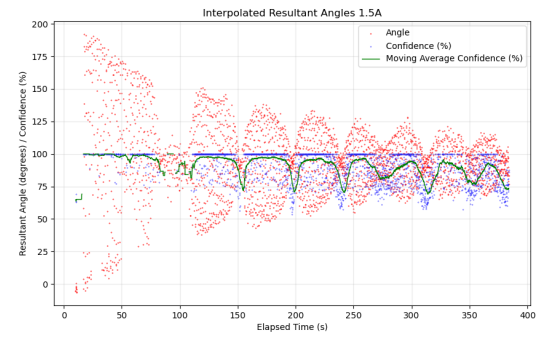


Figure 2: Live-tracked angular displacement over time as recorded by PYAXIOMA.

Figure 2, along with other plots generated during this experiment, provides critical insight into the dynamic behavior of the system under observation through the PYAXIOMA framework. As current is applied to the upper and lower coils, a magnetic field is established, which in turn exerts torque on the black magnetic marker affixed to the cue ball. With an airflow mechanism in place to reduce (though not entirely eliminate) friction, the cue ball is free to undergo rotational motion. This motion manifests primarily as an oscillation, bearing strong resemblance to a damped harmonic oscillator.

Interestingly, I observed an additional mode of motion—precession—where the axis about which the cue ball rotates gradually shifts over time. In my trials, the marker precessed by approximately 90° over a span of 50 seconds. This unexpected behavior significantly complicates the interpretation of angular displacement from a single camera view. As a result, my setup alone proved insufficient for capturing the complete dynamics of the system. To overcome this limitation, Lucciana and I developed complementary image processing pipelines, PYAXIOMA-JH and PYAXIOMA-LC ([Caceres Holgado 2025](#)) in conjunction, and placed our respective cameras at a 90° offset. This dual-camera configuration allows us to maximize the accuracy and temporal resolution of the

angular data by capturing projections from orthogonal planes.

In examining Figure 2, the presence of damped harmonic motion is immediately apparent. The envelope of the oscillations decays in a pattern characteristic of exponential damping, following a form similar to e^{-t} .

Superimposed on this decay, however, is a sinusoidal trend not attributable to the expected torque response. Initially, I hypothesized that this sinusoidal component originated from the torque function itself, which varies with $\mu \times B \sin \theta$. Upon further inspection, I realized that the observed sinusoidal shape arises from precessional motion. Because the data shown in Figure 2 represent a two-dimensional projection, the effect of precession appears as a sinusoid in the measured angle, even though the true spatial trajectory is more complex.

The sinusoidal signature arising from the torque function is not captured in this view alone. It emerges only when both data sources—my camera and Lucciana’s orthogonal system—are considered together. By combining our datasets, we obtain a more complete three-dimensional understanding of the cue ball’s orientation and how the torque evolves in response to the applied magnetic field.

UTC Time	Angle (deg)	Confidence (%)
20:02:58.151	24.10	89.22
20:02:58.250	58.07	88.41
20:02:58.349	98.13	86.97

Table 1: Sample data from 1.5A measurements. UTC time is given to be on 2025-04-17, and all following values are rounded to 2 decimals

4. DISCUSSION

The results indicate that PYAXIOMA is capable of measuring angular displacement with astonishing precision using only a consumer-grade camera and open-source libraries. The confidence metric, which integrates mo-

tion energy, stability, and spatial fidelity, was a useful tool for filtering low-quality frames and improving data reliability.

One of the key limitations observed was the reliance on marker motion for detection. In frames where the black marker remained static, no angle was computed. While this limitation aligns with the assumptions of torque-induced rotation, it could limit use cases involving steady-state angular positions.

Another consideration is environmental sensitivity. Lighting inconsistencies and background color significantly affected segmentation performance. These issues can be mitigated with better-controlled experimental environments and calibrated HSV thresholds.

The successful integration of confidence scores, real-time overlays, and automated data logging makes this method viable for small-scale laboratory experiments involving angular motion tracking. It may also be extendable to rotational dynamics studies in undergraduate physics labs or remote sensing systems where affordability and flexibility are critical.

5. CONCLUSION

I have proposed a low-cost, accessible method for measuring angular displacement without physical contact using computer vision. The pipeline relies on common hardware and open-source software. Ongoing work will calibrate and validate this approach experimentally.

¹ I would like to thank the University of Kansas and
² the support of Jessy Changstrom and Cole Douglas Le
³ Mahieu for their continued support in this Software de-
⁴velopment.

Software: OpenCV, PYAXIOMA, NumPy, Matplotlib

Data and Code Availability: All raw data, analysis scripts, and software source code are publicly available at: <https://github.com/JHavens2187/PYAXIOMA-JH>.

REFERENCES

- Caceres Holgado, L. 2025
- Department of Physics and Astronomy. 2024, Magnetic Torque Student Manual, University of Kansas
- Gonzalez, R. C., & Woods, R. E. 2002, Digital Image Processing, 2nd edn. (Prentice Hall)
- Hu, M.-K. 1962, IRE Transactions on Information Theory, 8, 179, doi: [10.1109/TIT.1962.1057692](https://doi.org/10.1109/TIT.1962.1057692)
- Piccardi, M. 2004, in Proceedings of the IEEE International Conference on Systems, Man and Cybernetics, IEEE, 3099–3104, doi: [10.1109/ICSMC.2004.1400815](https://doi.org/10.1109/ICSMC.2004.1400815)
- Smith, A. R. 1978, in Proceedings of the 5th Annual Conference on Computer Graphics and Interactive Techniques (SIGGRAPH ’78) (ACM), 12–19
- Yuen, H., Princen, J., Illingworth, J., & Kittler, J. 1990, Image and Vision Computing, 8, 71, doi: [10.1016/0262-8856\(90\)90059-E](https://doi.org/10.1016/0262-8856(90)90059-E)